

MISSION REPORT

***PROJECT: GEOID UNDULATION MODEL
BHUTAN***

FINAL REPORT

Prepared by:

Rui Fernandes

Machiel Bos

*Serpins, Portugal
7 July 2015*

Index

Pg.

1. Introduction	3
1.1 Summary	3
1.2 Motivation	3
1.3 Height Systems	4
1.4 Global Geopotential Models.....	7
2. Data used	12
2.1 Gravity observations	12
2.2 GNSS data	13
2.3 Absolute gravity point	14
2.4 Digital Terrain Model.....	15
3. Regional geoid computation.....	17
3.1 Remove-Restore technique.....	17
3.2 Residual Terrain Correction	18
3.3 Least-Squares Collocation	21
3.4 Height anomaly to geoid undulation conversion	25
3.5 Restore step	28
3.6 Synthetic tests	28
4. Vertical datum	32
5. Conclusions and Recommendations.....	34
5.1 Conclusions	34
5.2 Recommendations	35
6. Digital Annexes	36
7. References	37

1. Introduction

1.1 Summary

This document contains the final report to be submitted in the framework of the DRUKGEOID2015 project, which has the goal of compute the new Bhutanese geoid undulation model.

It summarizes the work done (partially already presented in the previous report) in order to compute the DRUKGEOID2015 model. It also proposes methodologies and best-practices to implement it in order that will be a fundamental instrument for the development of Bhutan.

We deeply thank NLC (National Land Commission) for all continuous support, in particular to the members of the NLC staff that collaborate in this project, both at office and field, in particularly:

1. Kinzang Thinley, Specialist.
2. Jamphel Gyeltshen, Surveyor.
3. Sangay Dorji, Surveyor.

1.2 Motivation

The zero height reference surface is normally defined to coincide with mean sea level. In countries without access to a coastline with tide gauges, the realization of such a height datum cannot achieved directly. The traditional solution is to transport the zero height datum from a tide gauge to benchmarks distributed over the country by geodetic levelling. The height of any point can then be determined by observing the height difference with one of these benchmarks. Although geodetic levelling is a very accurate geodetic technique, it is expensive and very time consuming. In addition, the benchmarks need to be maintained over the years.

An alternative to geodetic levelling is to measure the gravity field over the area of interest that can be converted into a potential field. Such a potential field is called a geoid and has the property that it coincides, except for an arbitrary vertical offset, with mean sea level in the absence of ocean currents. This method does not require access to a tide gauge and is therefore suitable for Bhutan.

Another geodetic technique to measure heights is the Global Navigation Satellite System (GNSS). With a geodetic GNSS receiver one can obtain centimeter level accuracy for any given point with a clear view of the sky. However, GNSS provides heights above the reference ellipsoid, such as WGS84, which is a geometrical shape that has been fitted to the Earth. Since official heights are given with respect to mean sea level, a geoid model is still required to convert the ellipsoidal heights into heights above mean sea level.

In this report we discuss the computation of such a regional geoid model, called DRUKGEOID15, using the terrestrial gravity data that were recently collected by the National Land Commission of Bhutan over large parts of the country.

1.3 Height Systems

The objective of geodetic levelling is to measure the difference in height between two points and is performed by summing the height differences, Δh , observed along various segments between the start and end point of the levelling line, see Figure 1. These heights are always measured vertically, or in other words, along the direction of gravity. If gravity is changing between the start and end point of the levelling line, then this will influence the results obtained. To avoid that the chosen track between the start and end point, say points A and B, of the levelling line has an effect on the obtained height difference, also the gravity g along

the track is observed. Together with the observed height differences, these are used to compute potential differences:

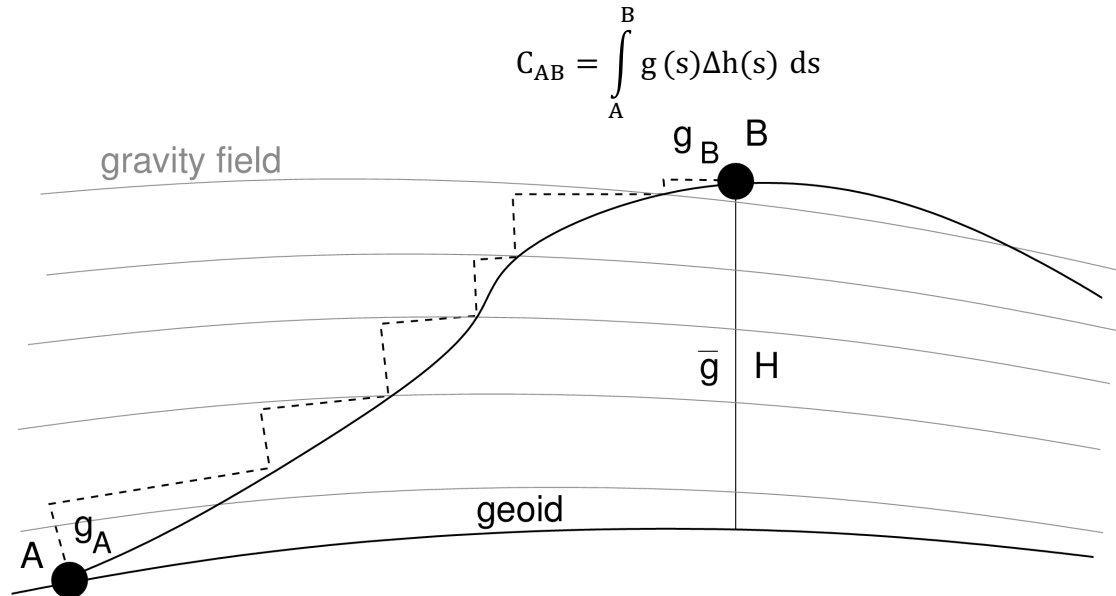


Figure 1 – Schematics of levelling between point A and B

If we assume that point A is at sea level, then the height of point B is:

$$H = \frac{C_{AB}}{\bar{g}}$$

where \bar{g} is the mean gravity value between point B and sea level, see **Error! Reference source not found..** Using this equation results in so called orthometric heights. A difficulty that arises is that one does not know the exact mean gravity value between point B and sea level. For that reason, one sometimes replaces the mean gravity with the mean normal gravity $\bar{\gamma}$ that is produced by the reference ellipsoid (WGS84). The results are called normal heights:

$$H^N = \frac{C_{AB}}{\bar{\gamma}}$$

According to Vaníček, Kingdon, and Santos (2012), normal heights are used in the countries of the former Soviet Union and 9 other European

countries (France, Germany, Sweden, Poland, Czech Republic, Slovak Republic, Hungary, Romania and Bulgaria).

The normal heights are given above the ellipsoid and form the telluroid. The separation between the telluroid and the Earth's surface are called height anomalies ζ . Orthometric heights H are given above the geoid while the geoid is referred to the ellipsoid by geoid undulations N . All these relations are given in Figure 2.

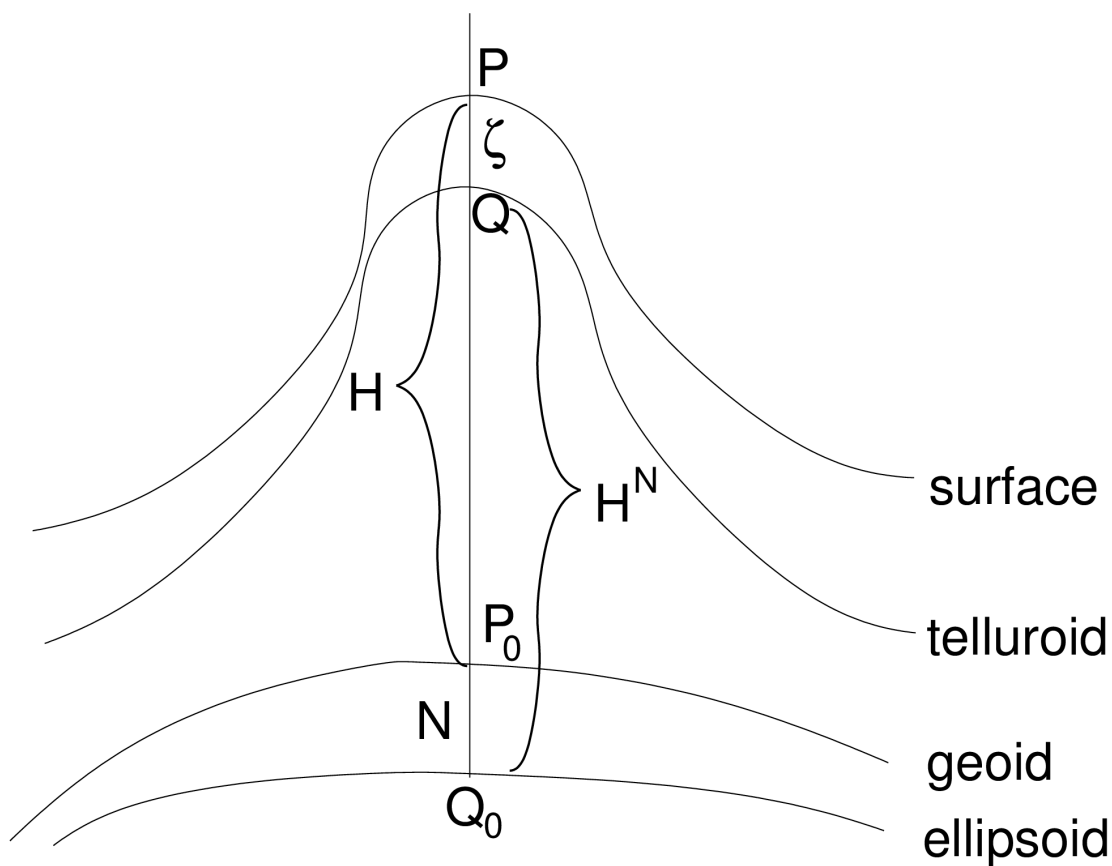


Figure 2 – The definition of the orthometric height H , the geoid undulation N , the height anomaly ζ and the normal height H^N .

Note that we have the following relation:

$$N + H = \zeta + H^N$$

Using the previous relations, this can be rewritten as:

$$\zeta - N = \frac{\bar{g} - \bar{\gamma}}{\bar{\gamma}} H$$

This equations shows that we can first compute the height anomalies ζ and afterwards, using the correction shown on the right side of the previous Eq., convert those into real geoid undulations N . This is the approach followed in this report.

The first reason for this approach is that the Global Geopotential Models (GGM's) such as EGM2008 (Pavlis et al. 2012) and EIGEN-6C4 (Förste et al. 2011) are only valid outside the Earth's surface. A GGM consists out of a set of coefficients that can be used to compute a gravity field and a height anomaly field for any place on Earth. For the local geoid discussed in this report the long gravity/height anomaly wavelengths come from these GGM's which are in turn based on the satellite observations from GRACE and GOCE. The shorter wavelengths come from our terrestrial gravity observations. Height anomalies are computed on the surface where the GGM's still can be applied. The EGM2008 model also provides $\zeta - N$ corrections which will be discussed later on in this report.

We will use the differences between the real gravity observations and those computed using a GGM to compute a correction to the height anomalies of the GGM. This is the so-called remove-restore technique (Sjöberg 2005). These corrections can also only be computed outside the Earth's surface.

1.4 Global Geopotential Models

The recent years has seen a dramatic increase of the accuracy of global geopotential models (GGM's) due to the satellite missions GRACE and GOCE. These models can be used to compute the gravity field and height anomalies to wavelength as short as 150 km (Spherical Harmonic degree

200). One could wonder if these GGM's are already not good enough to be used for representing the geoid/height anomalies over Bhutan.

Two recent GGM's that have high spatial resolutions of 15-20 km are EGM2008 (Pavlis et al. 2012) and EIGEN-6C4 (Förste et al. 2011). The differences of their height anomalies are shown in Figure 3. It can be seen that the Himalayas are an area where still differences can be found in the order of a few meters. For Bhutan, the height anomalies for EGM2008 are shown in Figure 4 and its difference with EIGEN-6C4 is shown in Figure 5.

The corresponding figures for gravity (for a height of 1000 m) are shown in Figure 6 and Figure 7. The gravity field presented in Figure 6 has a large correlation with the topography shown later in Figure 9. One can conclude that even using the latest GGM's, an uncertainty of about ± 70 cm still exists for the height anomaly and around ± 20 mGal for the gravity. The reason for this misfit is that the satellite data needs to be complemented with satellite altimetry and terrestrial gravity observations. In areas where no such observations exists, as is the case for Bhutan, the errors are still large.

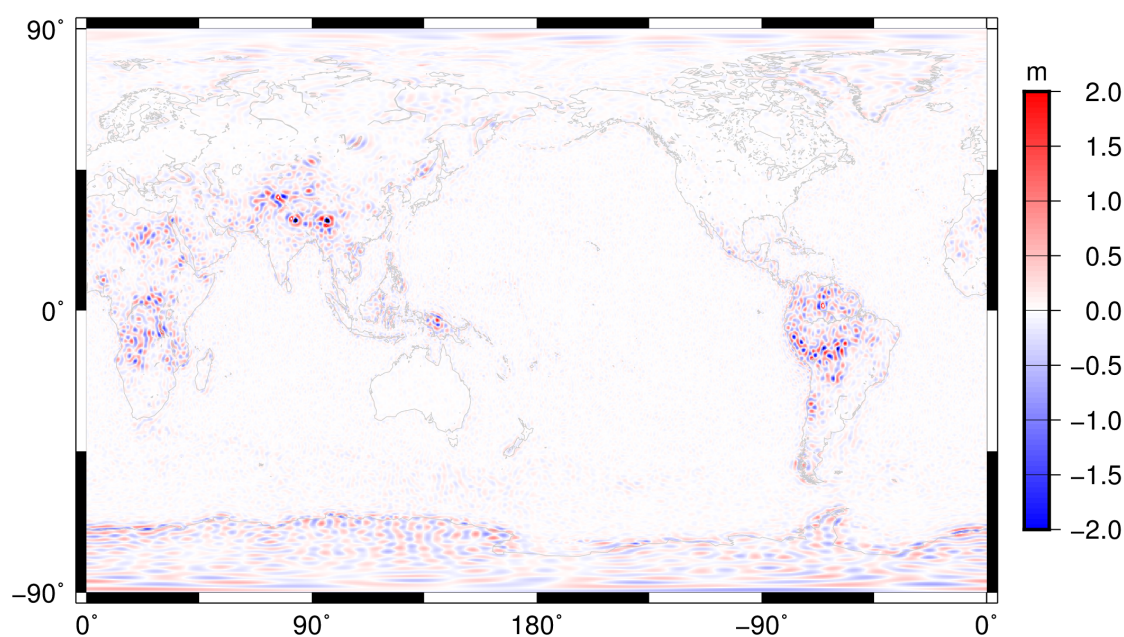


Figure 3 – The difference in height anomalies, computed using EGM2008 and EIGEN-6C4 globally.

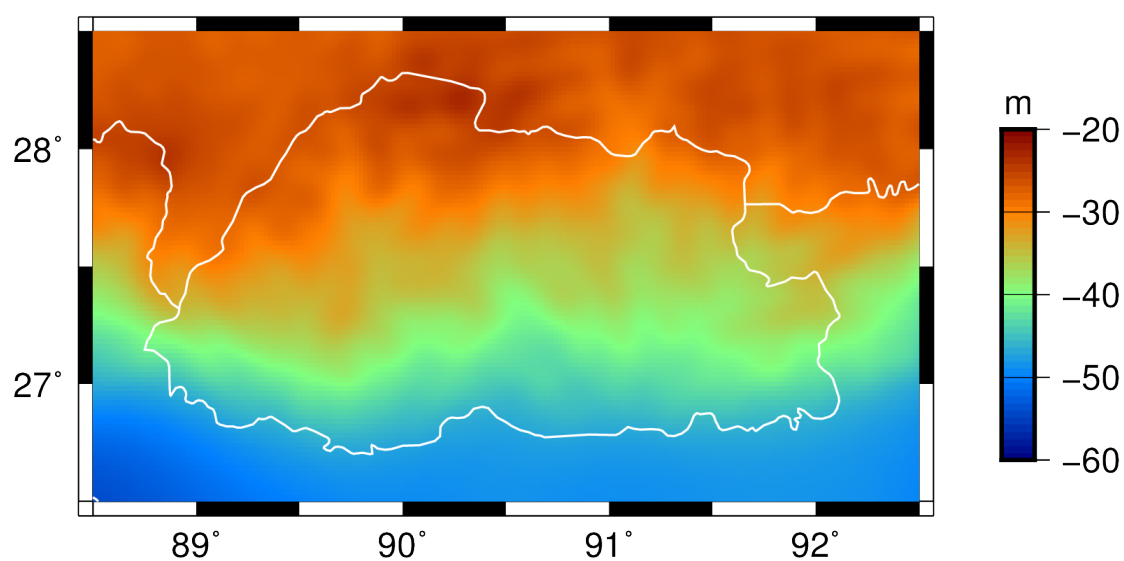


Figure 4 – The height anomalies, ζ_{GGM} , computed using EGM2008 over Bhutan.

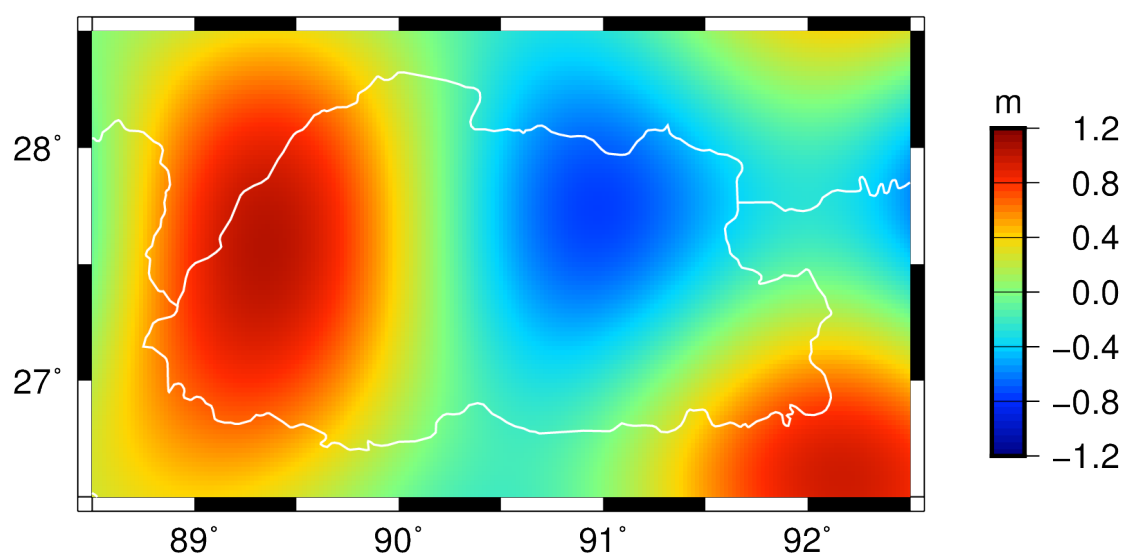


Figure 5 – The difference in height anomalies, computed using EGM2008 and EIGEN-6C4.

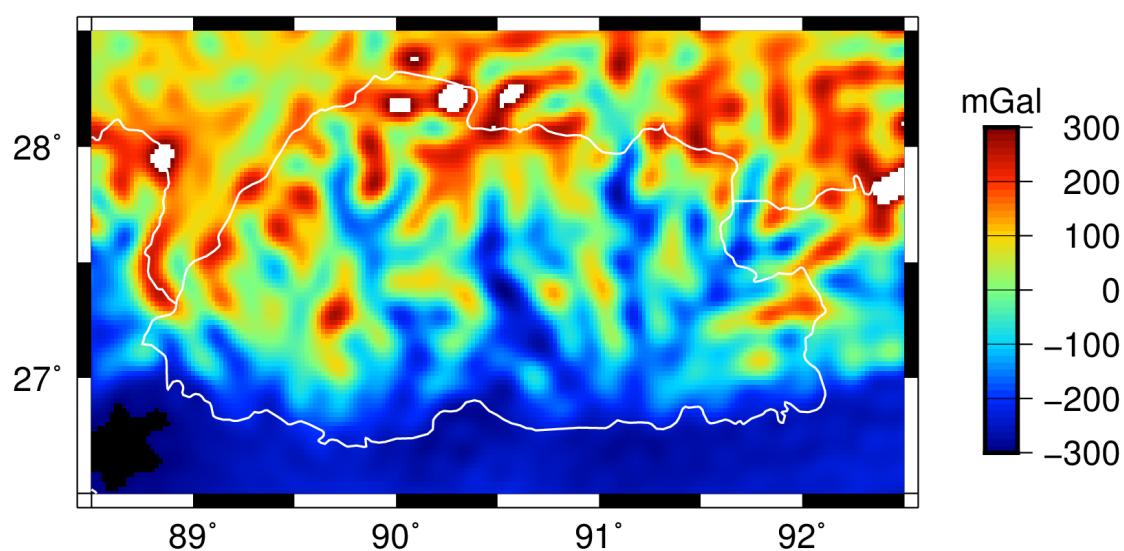


Figure 6 – The gravity, g_{GGM} , computed using EGM2008 over Bhutan minus 978900 mGal at a height of 1000 m.

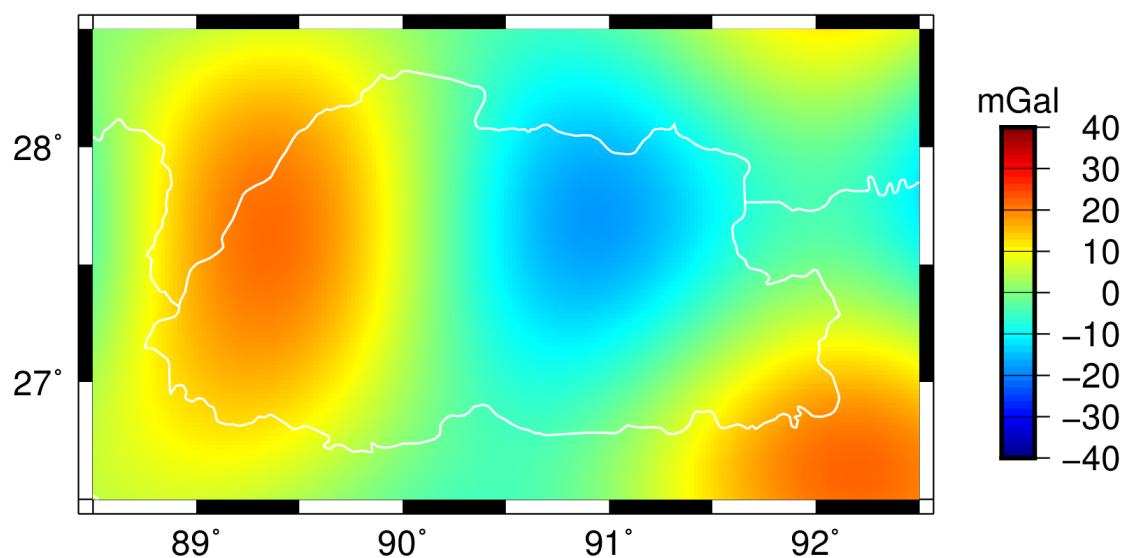


Figure 7 – The difference in gravity, computed using EGM2008 and EIGEN-6C4 at a height of 1000 m.

2. Data used

2.1 Gravity observations

Gravity observations were observed by NCL using two SCINTREX CG5 gravimeters from November 2014 to May 2015. In the current campaign a total 271 gravity points were observed. At 16 points no GNSS observations were possible which resulted in a set of 255 points with both GNSS and gravity that are shown in Figure 8. In this figure the color of each point indicates the number of times it was re-observed. Points that have been re-observed more than once help to constrain the drift of the instruments and provide an estimate of the repeatability.

The gravity data from the two gravimeters were corrected for the solid Earth tide and a quadratic drift rate was assumed in the processing. The first months the gravimeters suffered from battery problems which caused some erroneous measurements. The reason is that the instruments cool down when the battery is empty and they need some hours to recover to its original condition, even when new batteries are meanwhile inserted into the instrument. In the preprocessing phase all measurements that were made with an instrument temperature of more than 0.02 Kelvin from the nominal value were omitted. Also observations that had a tilt value larger than 50 arc seconds from horizontal or a duration of less than 10 seconds were ignored.

The battery problems produced a standard deviation of around 0.7 mGal for observations before February 2015. After this problem was diagnosed and new batteries were bought in the scope of this project, the standard deviation of the network solution reduced to around 0.3 mGal.

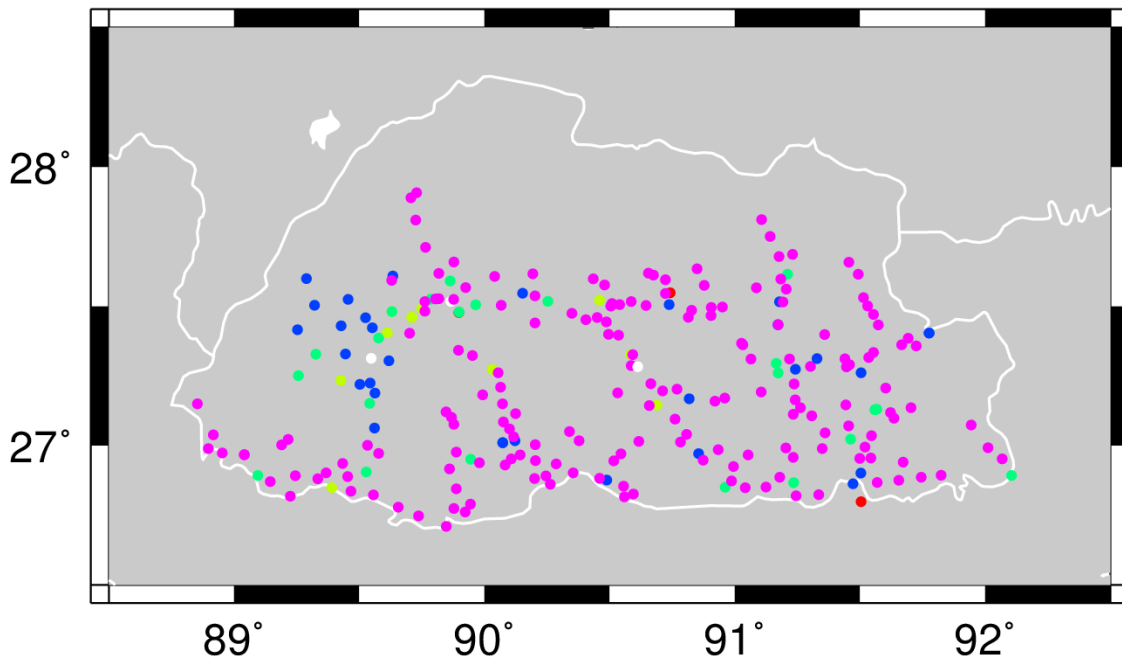


Figure 8 – The 251 observed gravity/GNSS points. The colour indicates the amount of reobservations. Pink=1, Blue=2, Green=3, Yellow-Green=4 and Red=5.

2.2 GNSS data

GNSS observations at the gravimetric points are also required to be able to know their horizontal location and ellipsoidal height. Gravity decreases by about 0.3 mGal/m for increasing height and if the ellipsoidal height is not determined accurately it is impossible to determine if a change in observed gravity between two points is caused by variations in the density of the rocks underneath the surface or if it is caused by an error in the observed height. Before the existence of the GNSS technique, the heights of the gravity observations were taken from topographic maps or using a barometer and these were one of the largest source of error in the geoid computation process.

A mean observation period of 1 hour was acquired at all points. The vertical offsets of the GNSS antenna and gravimeter was measured in order to use the ground as reference surface.

For points for which nearby GNSS data from the Permanent Reference Stations (PRS's) were available the positions were computed using the differential GNSS approach and the Trimble Business Center software. The PRS were used as known points that were fixed into the international reference frame (ITRF2008).

When no PRS was available within 50 km, alternative online systems using the Precise Point Positioning technique were employed. These were NRCAN and APPS that can be found at: <http://webapp.geod.nrcan.gc.ca/geod/tools-outils/ppp.php> and <http://apps.gdGNSS.net>

During the campaign various points were observed more than once. In addition, some points could be analyzed with TBC, while others with APPS/CSRS and some by both. The final GNSS solutions were computed by taking a weighted mean of all solutions.

The methodologies used to compute the ellipsoidal height at all points are discussed in very detail in Report 1, that was delivered after the first visit of Rui Fernandes and Machiel Bos in February 2015.

2.3 Absolute gravity point

All observations made during the gravity campaign are relative observations. That is, they only provide differences in gravity between points. To convert these into absolute gravity values, at least at one point the absolute gravity should be known. In Bhutan we used the absolute gravity point at the headquarters of NLC that is linked to the Indian gravity network. To ensure that in case this point disappears, other points can be used to recover the absolute value, NLC made a small number of gravity measurements at their institute. The results are shown in Table 1.

Table 1 – Gravimetric points at NLC (unit mGal)

Description	Label	gravity value
Absolute point, below ground	TH01	978358.100
Absolute point, ground level	TH06	978357.915
Base of flag pole	TH02	978357.645
Near the entrance, on concrete	TH03	978357.684
Inside trigroom	TH07	978357.181
New absolute point room	TH08	978357.637

A new value of absolute gravity at TH08 was recently measured with a value of 978357.060 mGal which is only 0.6 mGal different from the value obtained using the current absolute point.

2.4 Digital Terrain Model

As was explained in Section 1.3, one needs to have a model of the topography to convert height anomalies ζ into orthometric heights H . In addition, removing the effect of the topography on the gravity observations results in a smoother gravity field with smaller variance that is beneficial for the height anomaly computation.

This topography has been taken from the Shuttle Radar Topography Mission (Farr et al., 2007) which has a spatial resolution of around 90 meters and is shown in Figure 4. SRTM gives the height above sea level while the geoid computation software expects height above the ellipsoid. The EGM96 geoid (N) was used to convert the orthometric heights H to ellipsoidal ones (h).

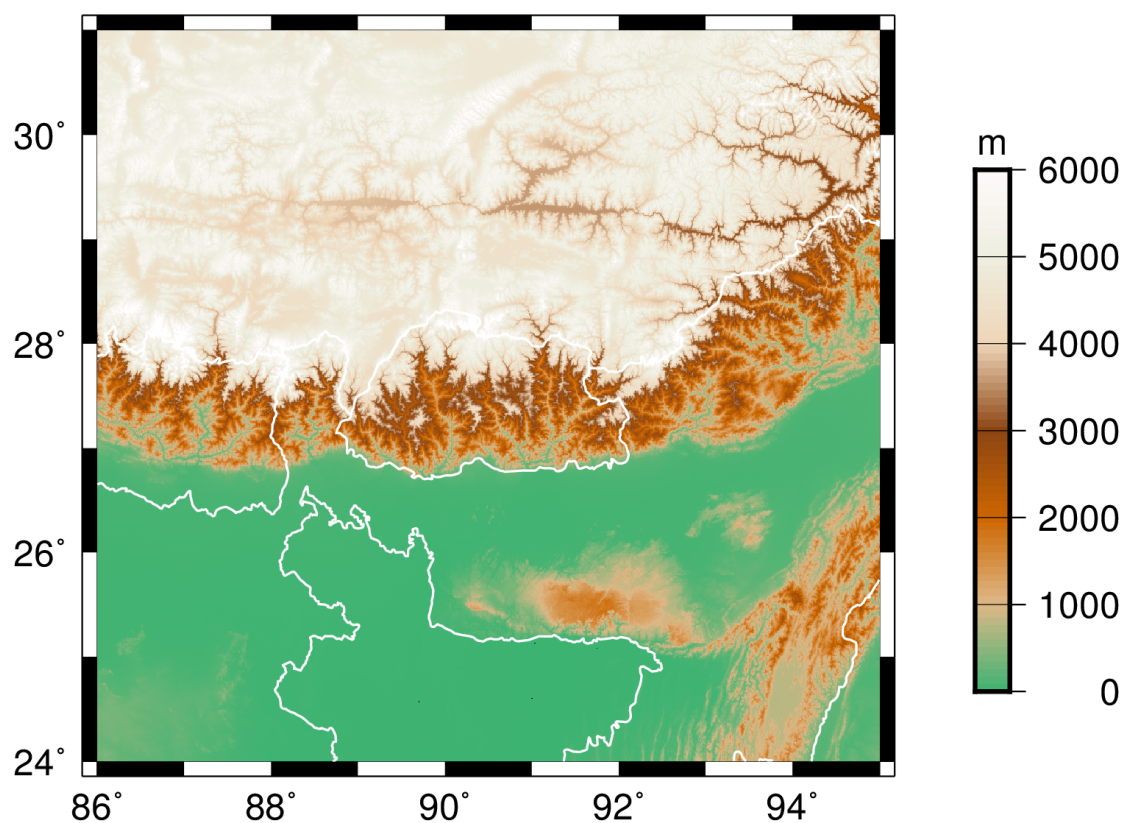


Figure 9 – The topography for Bhutan and its surroundings.

3. Regional geoid computation

3.1 Remove-Restore technique

We noted in Section 1.4 that current GGM's are not accurate enough to represent the geoid over Bhutan. However, they still are very useful as a first guess and the approach in this project is to compute corrections to the GGM's to make them more accurate. First, a GGM is used to compute the gravity at the observed points and the residual gravity values are then converted into height anomalies residuals. These are then added to the height anomalies generated using the GGM. This process is known as the Remove-Restore technique (Sjöberg, 2005).

EGM2008 and EIGEN-6C4 only predict the Earth's gravity/geoid field to a wavelengths of about 15-20 km. However, Bhutan is very mountainous and the shorter wavelengths of the topography still have a significant contribution to the gravity and geoid field. Therefore, another step in the remove-restore method is needed to remove the gravitational attraction from the observations and put them later back as to the height anomalies. To summarize, our remove step contains the following corrections to the gravity observations g_{obs} :

$$g_{res} = g_{obs} - g_{GGM} - g_{TC}$$

where g_{res} are the residual gravity values, g_{obs} the observed gravity values, g_{GGM} the gravity values computed using a GGM and g_{TC} the gravity effect caused by the short wavelength topography.

In the restore step we obtain the total height anomaly ζ by summing:

$$\zeta = \zeta_{GGM} + \zeta_{TC} + \zeta_{res}$$

where ζ_{GGM} is the height anomaly produced by the GGM, ζ_{TC} the height anomaly caused by the short wavelength topography and ζ_{res} is computed out of the residual gravity values g_{res} using Least-Squares Collocation.

The topographic correction and Least-Squares Collocation will be discussed in the next sections.

3.2 Residual Terrain Correction

To compute the contribution of the short wavelength topography on the gravity field and height anomalies, the SRTM topography was smoothed to remove the long wavelengths, assumed to be represented by the GGM, and the difference between the SRTM and the smoothed topography was used to compute the gravitational attraction on our observation points. This is better known as the residual terrain correction as developed by Forsberg and Tscherning (1981).

Since we assume that the long wavelength, down to 15-20 km, are represented by the GGM, it is associated with the smoothed topography. Since some observation points are underneath the smoothed surface, one needs to apply a correction to g_{GGM} to take this aspect into account.

The gravity residuals g_{res} after only subtraction the gravity field of EIGEN-6C4, g_{GGM} , from the observations are shown in Figure 10. For these computations a standard rock density of 2670 kg/m^3 was assumed. It shows gravity differences of up to $\pm 120 \text{ mGal}$ which is about three times larger than the differences between EGM2008 and EIGEN-6C4 shown in Figure 7. Figure 10 also shows a distinct pattern of two large regions with negative anomalies in the East and West with a region with positive anomalies in the middle. This pattern will reoccur in the computed residual height anomalies, ζ_{res} .

The residuals are subtraction the gravitational attraction, g_{TC} , of the topography with wavelengths shorter than 20 and 40 km are shown in Figure 11 and Figure 12. One can observe that for a cut-off wavelength of 20 km smaller residuals and a smoother gravity field is obtain. The standard deviation is reduced from 59 to 44 mGal. For the cut-off

wavelength of 40 km, the gravity field is still smooth but the variances are slightly larger. More statistics, also for other cut-off wavelengths are shown in Table 2.

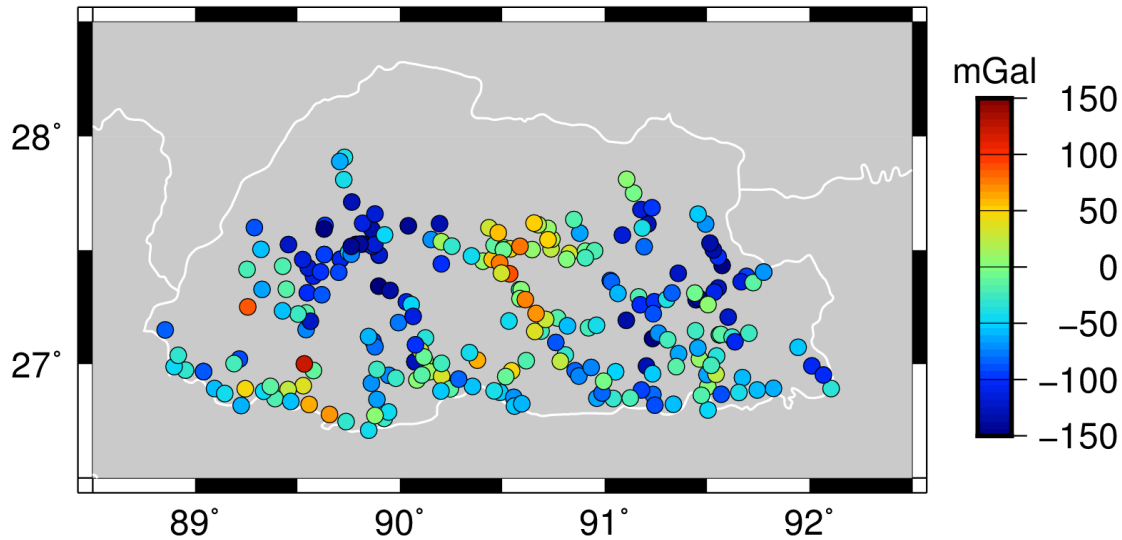


Figure 10 – The gravity observations (after subtracting EIGEN-6C4).

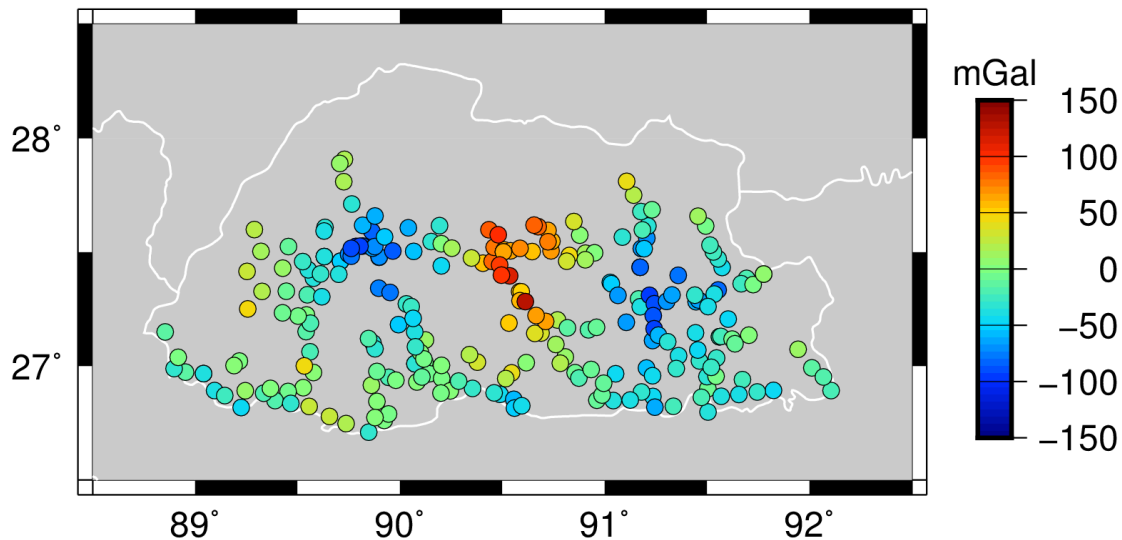


Figure 11 – The gravity observations (after subtracting EIGEN-6C4 and topography effect with wavelengths shorter than 20 km).

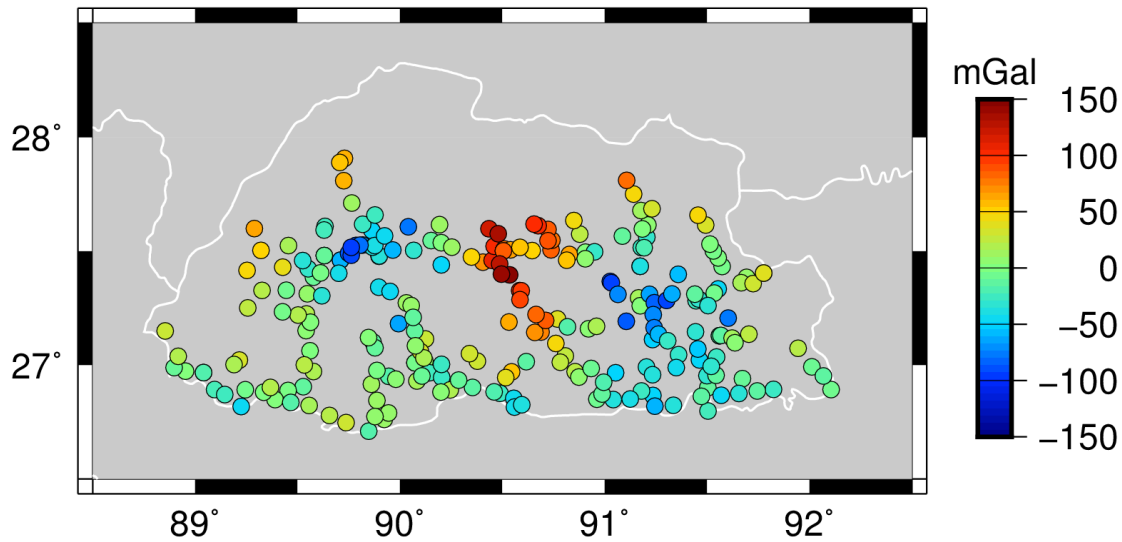


Figure 12 – The gravity observations (after subtracting EIGEN-6C4 and topography effect with wavelengths shorter than 40 km).

Table 2 - Statistics of applying the short wavelength topographic corrections to the observed gravity values g_{obs} from which the gravity field of EIGEN-6C4, g_{GGM} , has been subtracted (Units: cm).

Wavelength (km)	Mean	STD	Min	Max
No g_{TC}	-52	59	-191	122
10	-30	47	-177	105
20	-14	44	-170	127
30	-5	46	-162	142
40	0	49	-154	155

The contribution to the height anomalies due to topography effect with wavelengths shorter than 20 km are shown in Figure 13 and shows that they can reach ± 30 cm. Thus, even if the current errors in the GGM models EGM2008 and EIGEN-6C4 would be resolved, then they would still contain errors of this magnitude due to truncating the development of the spherical harmonic series to wave-lengths down to 15-20 km, ignoring the shorter ones.

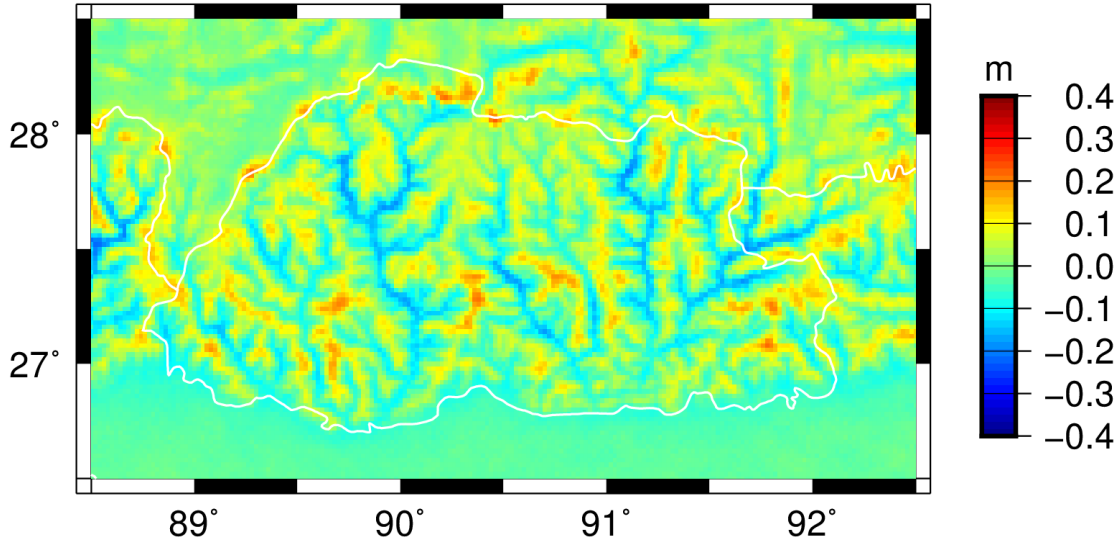


Figure 13 – The contribution to the height anomalies ζ_{TC} due to topography effect with wavelengths shorter than 20 km).

3.3 Least-Squares Collocation

So far we have subtracted from the gravity observations the contributions from the GGM and the short wavelength topography. This resulted in a smooth gravity field with a very reduced range of gravity variations. These gravity residuals, g_{res} were converted into height anomalies ζ_{res} using Least-Squares Collocation (LSC), see Moritz (1980). This theory assumes that the gravity field is random for which the spatial covariance function needs to be estimated. For some carefully chosen covariance models, the cross-covariance between gravity and height anomalies can be derived analytically once the parameters for the gravity covariance model have been determined.

Due to the availability of accurate ellipsoidal heights at the gravity points, we can work with gravity disturbances δg , which are defined as the observed gravity value at height h minus the normal gravity γ , also computed at height h :

$$\delta g = g_{obs}(h) - \gamma(h)$$

In our remove-restore method the normal gravity can be ignored which can be seen as follows:

$$\begin{aligned} g_{\text{obs}} - \gamma &= (g_{\text{GGM}} - \gamma) - g_{\text{TC}} - g_{\text{res}} \\ g_{\text{obs}} &= g_{\text{GGM}} - g_{\text{TC}} - g_{\text{res}} \end{aligned}$$

To estimate the sample covariance, the gravity residuals were interpolated to a regular grid with a spacing of 0.1 degrees. The estimated covariance function is shown in Figure 14. It shows that gravity is correlated in space to about 0.4 degrees, which corresponds roughly to 40 km. For larger distances gravity is anti-correlated. Through this sample covariance, the covariance model number 4 of Tscherning and Rapp (1974) was also fitted. The re-gridded residual gravity observations and the interpolated residual gravity field, computed using LSC, are shown in Figure 15. Due to the fact that the spatial covariance predicts that gravity is anti-correlated for distances larger than 40 km, a large negative region of gravity anomalies is created by LSC in the north-west. However, the reality of this region should be treated with caution since no gravity observations were made in this area. Figure 16 shows the uncertainty of the created gravity field and it shows that in areas where no observations exist, the uncertainty is large.

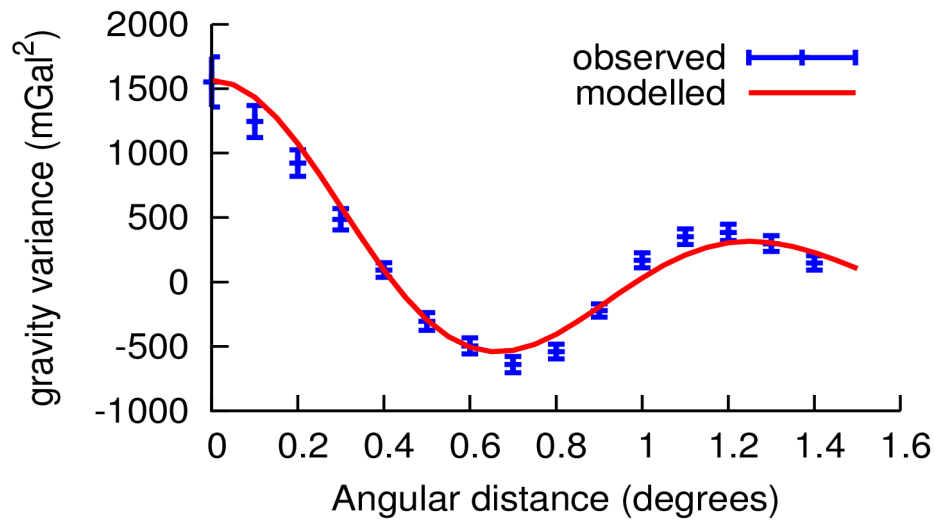


Figure 14 – Spatial covariance computed using the real observations (after subtracting EIGEN-6C4 and Topography effects). Through these sample covariance values we fitted a model which is also shown.

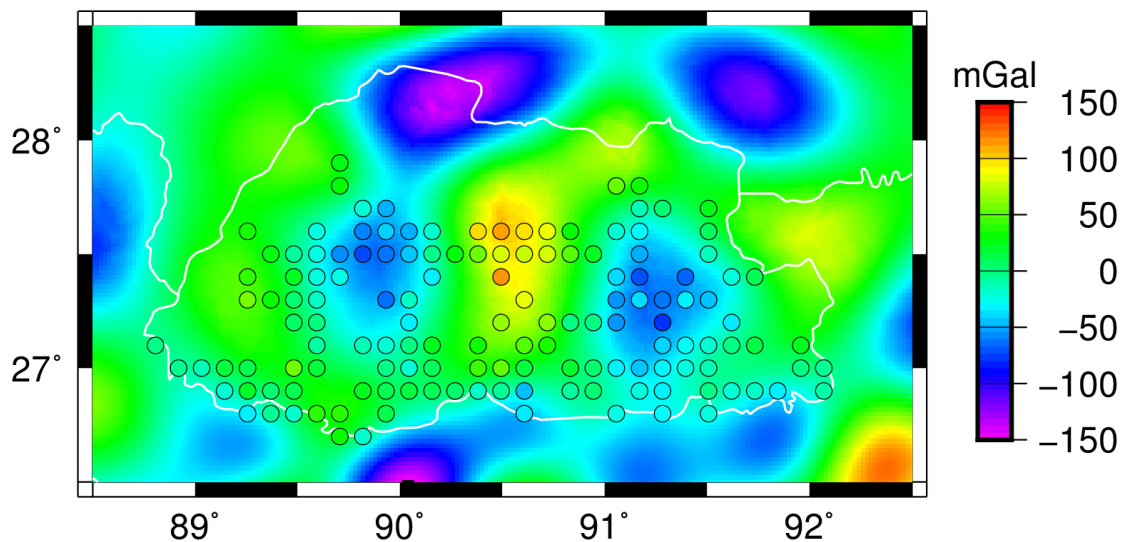


Figure 15 – The observed gravity residuals, regrided to a regular grid. LSC was used to create the interpolated gravity field

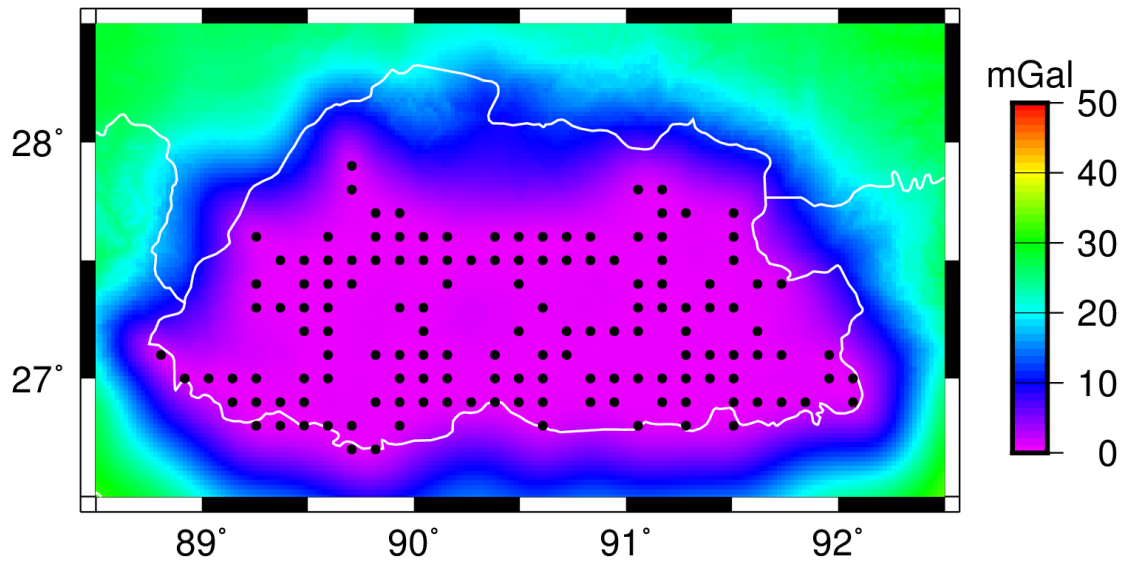


Figure 16 – The uncertainty of the interpolated gravity field generated with LSC.

Now that the parameters of the gravity covariance model have been estimated, the cross-covariance between gravity and height anomalies can be constructed and used to compute the height anomalies generated by the gravity residuals g_{res} . The result is shown in Figure 17 while its estimated uncertainty is shown in Figure 18. Note that height anomalies computed with LSC range from -1 to almost 2 meters which is substantial. This is the direct result of the large regions of negative and positive gravity anomalies shown in Figure 10, Figure 11, Figure 12, and Figure 15.

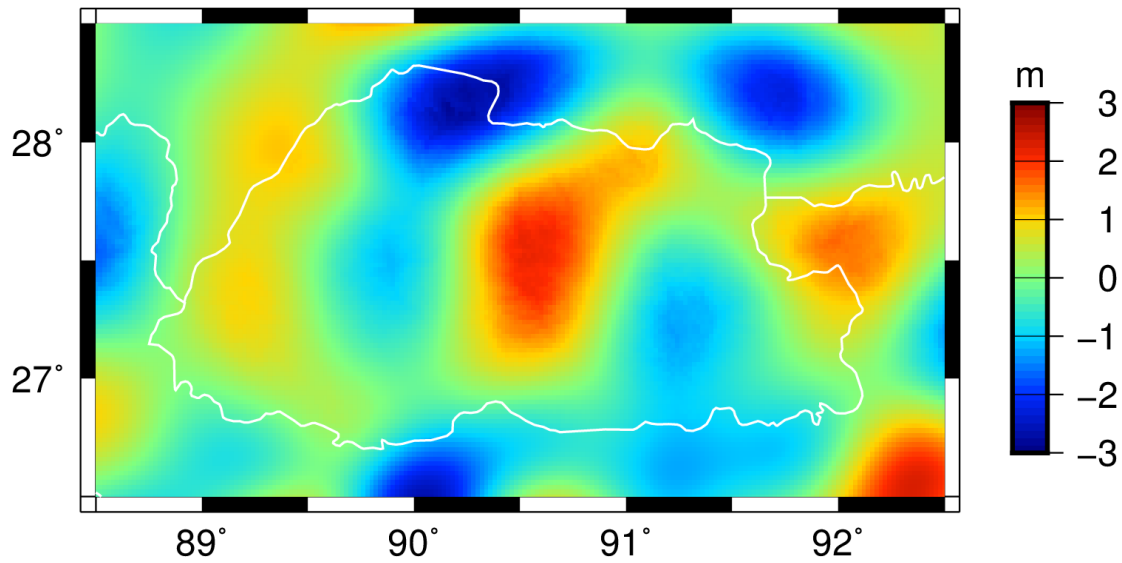


Figure 17 – The interpolated height anomalies generated with LSC

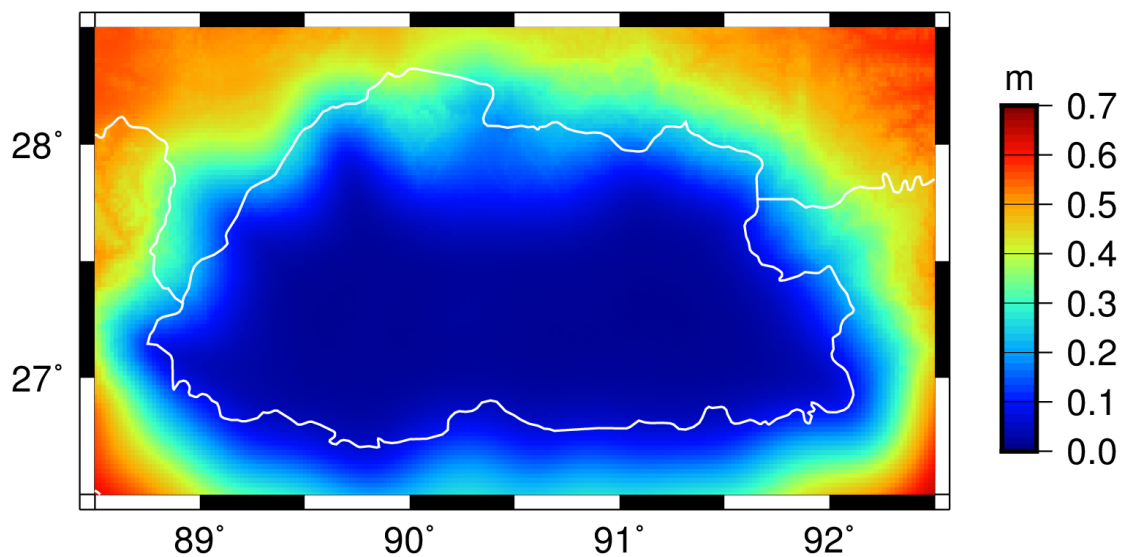


Figure 18 – The uncertainty of the interpolated height anomalies generated with LSC.

3.4 Height anomaly to geoid undulation conversion

As was mentioned in the Introduction, after computing the height anomalies they can be converted into geoid undulations once the mean gravity value \bar{g} between the surface and the geoid is known. The conversion formula is:

$$\zeta - N = \frac{\bar{g} - \bar{\gamma}}{\bar{\gamma}} H$$

From this conversion formula one can see that the differences between height anomalies ζ and geoid undulations N become larger for higher topography H . This is caused by the fact that the telluroid is defined near the surface and the geoid near the ellipsoid (cf. Figure 2). The larger their separation, the more these two surfaces will differ.

The authors of EGM2008 not only provided their GGM but also the correction to convert from height anomalies to geoid undulations. These are shown in Figure 18 and show corrections up to -3.5 m in the north due to the height mountains. However, they approximate in their calculations the topography at each point by an infinite plate. Flury and Rummel (2009) provided a more accurate algorithm for computing the conversion between height anomalies and geoid undulations that is shown in Figure 19. The differences with the corrections provided by EGM2008 is shown in Figure 20. Because the authors of EGM2008 simply assume that the topography at each point is simply a plate extending to all directions, they overestimate the corrections at the top of mountains (cf. Figure 21).

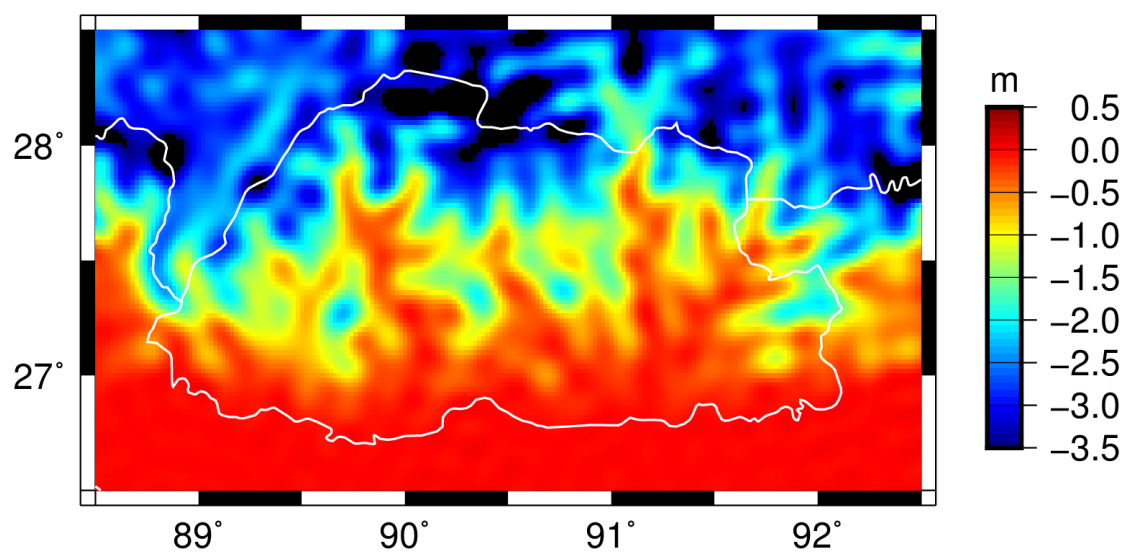


Figure 19 – The $N - \zeta$ corrections provided by the authors of EGM2008

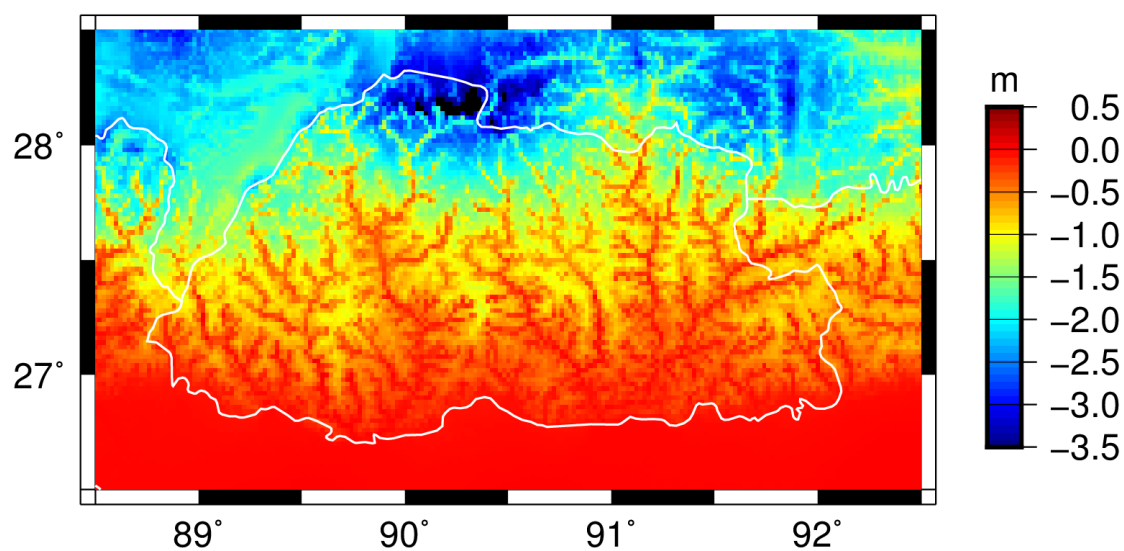


Figure 20 – The $N - \zeta$ corrections computed in the scope of this research

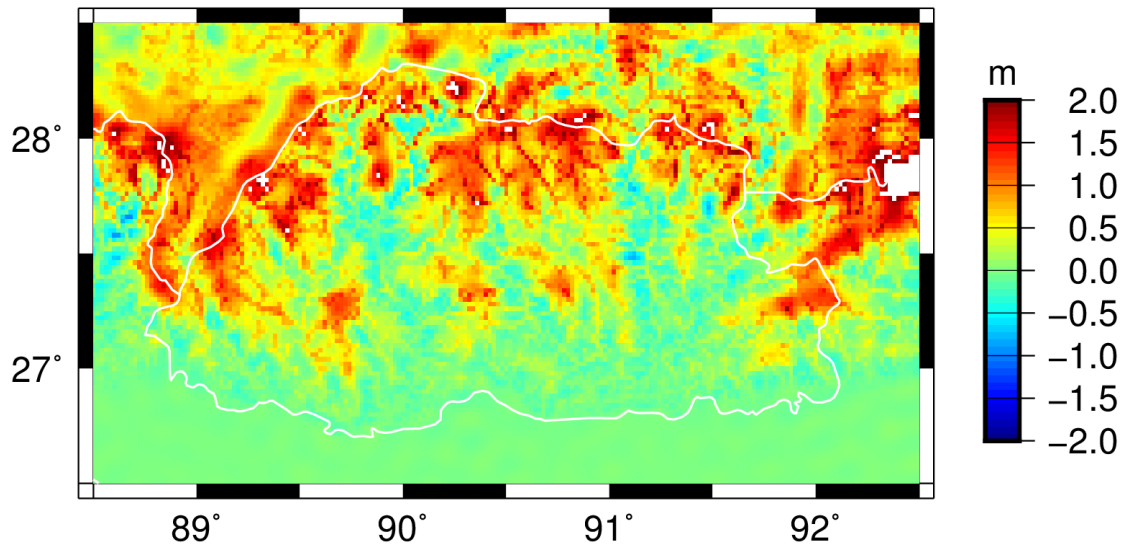


Figure 21 – The difference in $N - \zeta$ corrections computed in the scope of this project minus those provided by the authors of EGM2008

3.5 Restore step

At this moment we have computed the height anomalies due to the GGM, shown in Figure 4, the height anomalies due to the short wavelengths of the topography, shown in Figure 13, and the height anomalies due to the gravity residuals, shown in Figure 17. These should be added to obtain the total height anomalies. The difference of these total height anomalies with EGM2008 and are shown in Figure 18.

3.6 Synthetic tests

One way to estimate the accuracy by which the geoid can be computed is to create synthetic gravity observations at the actual observed points using a global geopotential model (GGM). Here we used the EIGEN-6C4 model (Förste et al., 2011). As before, we subtracted EGM2008 in the remove step. The gravity residuals are re-gridded to a regular grid and are shown in Figure 22. These gravity residuals will now be converted into height anomalies which should be, in the ideal case, be equal to the difference shown in Figure 2.

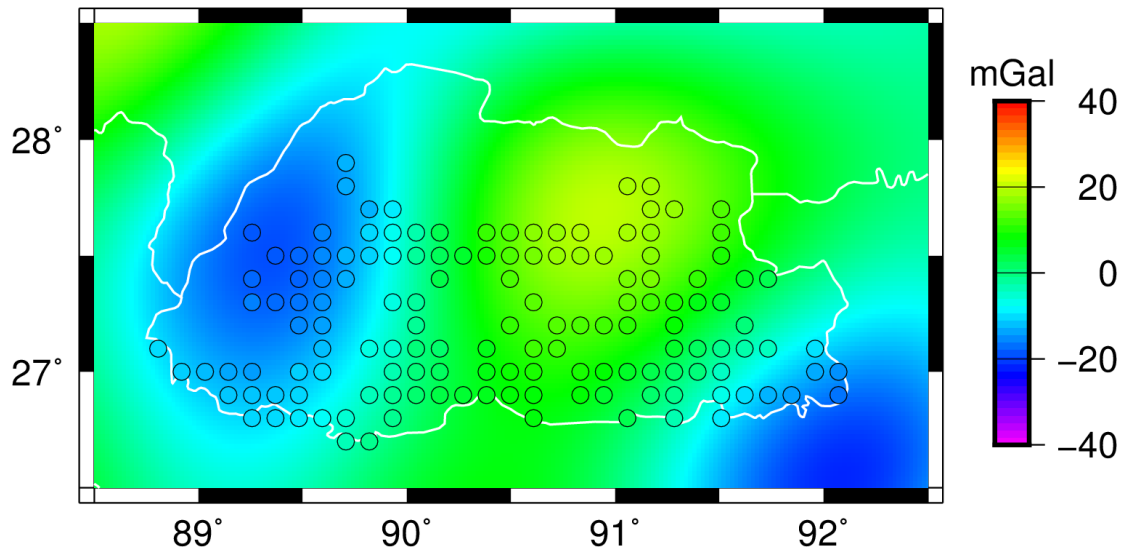


Figure 22 – The dots represent synthetic gravity observations, computed using EIGEN-6C4.

The spatial sample covariance is shown in Figure 23. To this sample covariance the covariance model of Tscherning and Rapp (1974) was fitted which is also shown in this figure. The Least-Squares Collocation (Moritz 1980) method was used to interpolate the gravity points to the whole area. This method was also used to compute the height anomalies due to the disturbing potential which are shown in Figure 24 and one can verify these are similar to those shown in Figure 2 as it should be. The difference is shown in Figure 25 and it can be concluded that for most of the country errors of ± 5 cm is obtainable and that the error grows rapidly near the borders where no observations have been made.

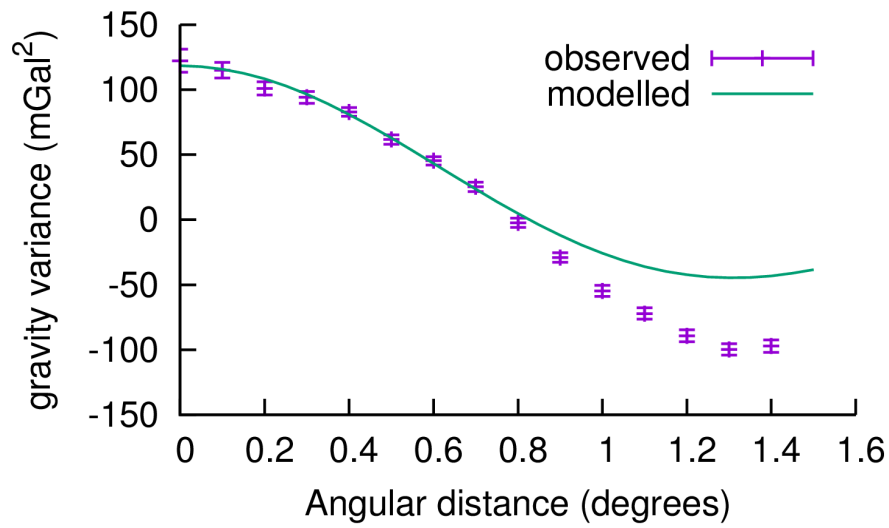


Figure 23 – Spatial covariance computed using the synthetic observations (after subtracting EGM2008). Through these sample covariance values we fitted a model which is also shown.

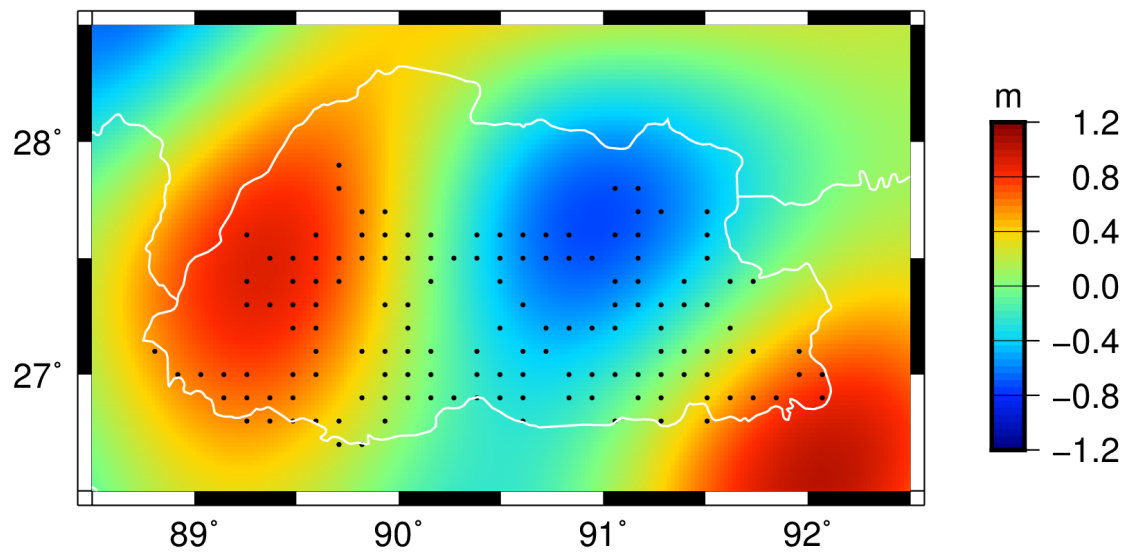


Figure 24 – The residual height anomalies computed using Least-Squares Collocation

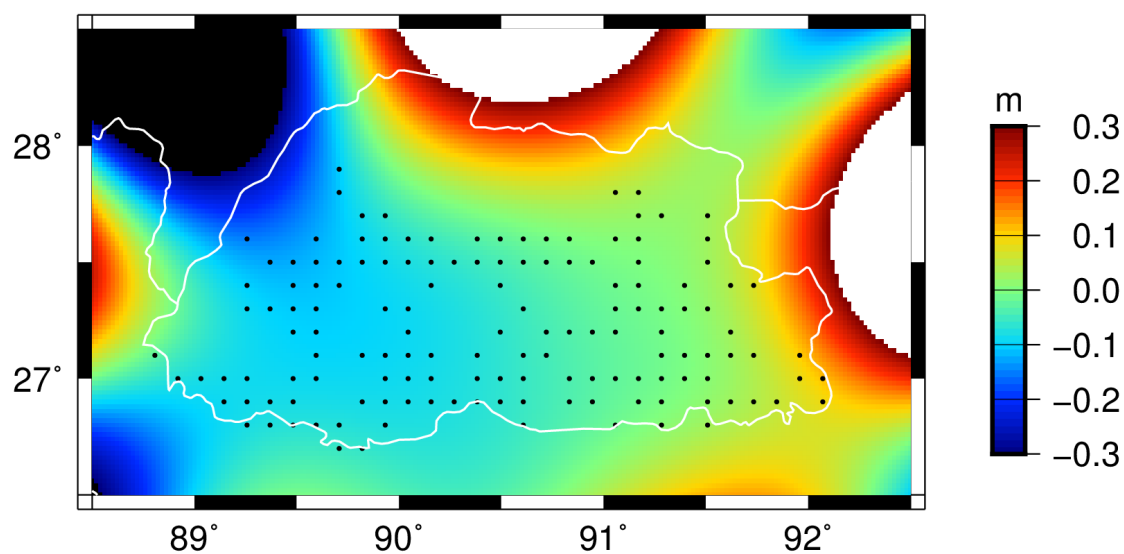


Figure 25 – The difference between the real difference between the height anomalies computed using EIGEN-6C4 and EGM2008 and obtained with Least-Squares Collocation

4. Vertical datum

We assume that the long wavelengths of the height anomalies are provided by the GGM's while the short wavelengths are computed from the gravity observations. This implicitly means that the GGM's determine the vertical datum of the computed height anomaly field and thus of the computed geoid. To be precise, to compute the GGM height anomalies one has to provide the potential value of the telluroid. So far we have chosen this value to be equal to the potential of the WGS84 reference ellipsoid ($62636851.71457 \text{ m}^2/\text{s}^2$) but other choices are possible. As Smith (1998) clearly pointed out, there is no unique value.

In other words, so far we have computed variations in the geoid that still need to be shifted up or down by an arbitrary offset in order to fit them to the national datum of Bhutan.

After discussion with NLC it was decided to fix the new geoid to the fundamental benchmark at NLC headquarters in Thimphu. The code of this benchmark is TH01. At this point the GNSS ellipsoidal height minus the new geoid undulation at TH01 is exactly to the official orthometric height of this point.

To ensure that the vertical height datum of the new geoid is accurate, more GNSS observations were made at this point and it was concluded that the ellipsoidal height has an accuracy of around 1-2 cm.

Furthermore, the DRUKGEOID15 and EGM2008 were compared to 27 GNSS/levelling points. The results of this comparison are shown in Table 3 and demonstrates the superiority of the new geoid over EGM2008. The actual differences with EGM2008 and DRUKGEOID15 are shown in Figure 26 and Figure 27.

Table 3 - Statistics of the comparison of DRUKGEOID15 and EGM2008 with 27 GNSS/levelling points.

<i>Geoid</i>	<i>MEAN(m)</i>	<i>STD(m)</i>	<i>MIN(m)</i>	<i>MAX(m)</i>
DRUKGEOID15	0.46	0.55	-0.71	1.71
EGM2008	1.90	1.70	-0.03	5.40

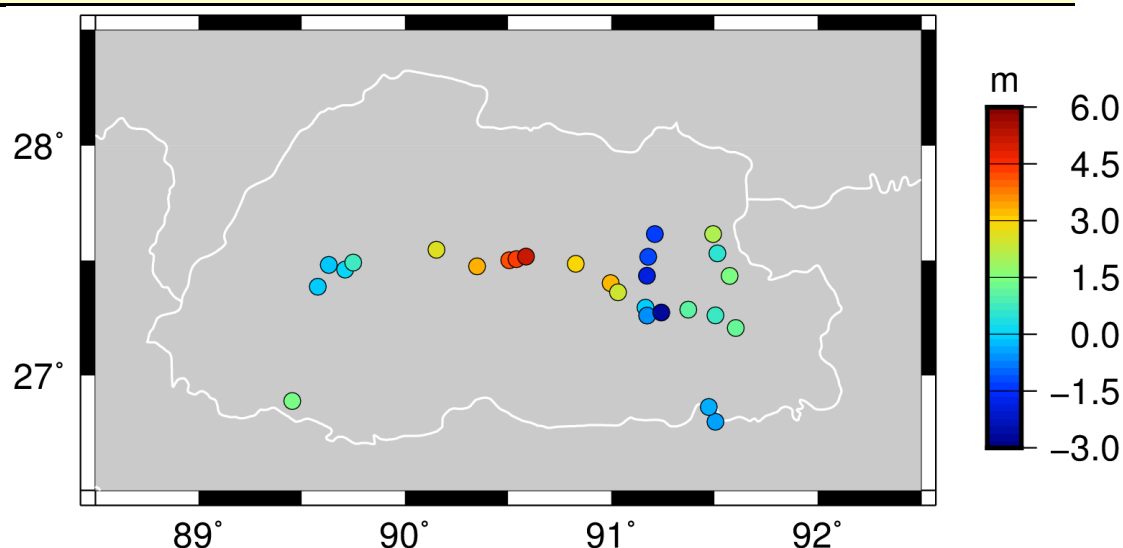


Figure 26 – The differences between EGM2008 and 27 GNSS/Levelling benchmarks

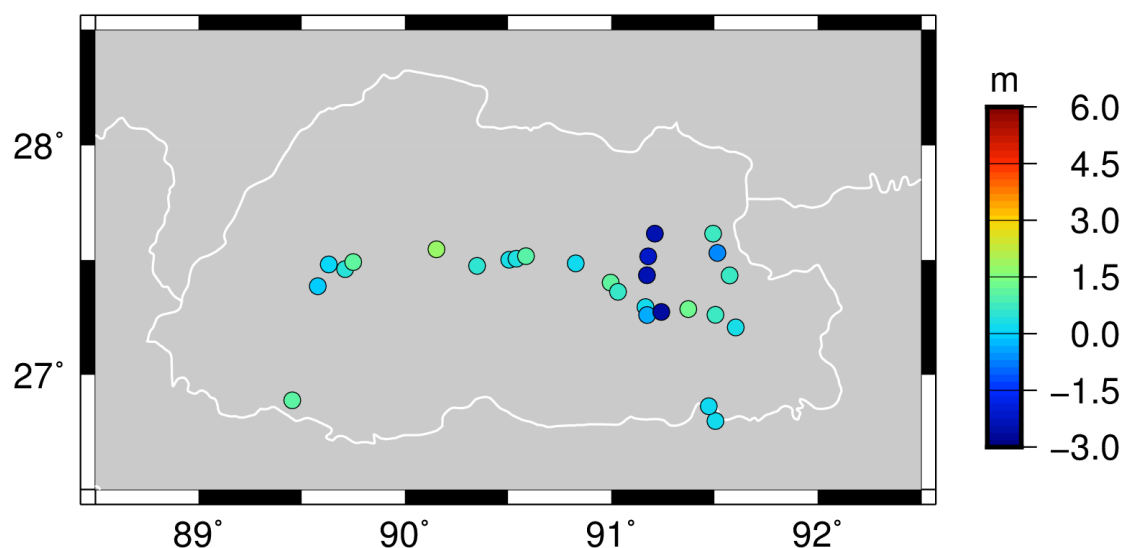


Figure 27 – The differences between DRUKGEOID15 and 27 GNSS/Levelling benchmarks

5. Conclusions and Recommendations

5.1 Conclusions

Recent Global Geopotential Models such as EGM2008 and EIGEN-6C4 still differ by about 50-80 cm over parts of Bhutan. For that reason a terrestrial gravity campaign was performed by the National Land Commission of Bhutan to compute a new local gravity geoid called DRUKGEOID15. During this campaign 272 gravity and GNSS observations were observed over the country with an average spacing of 10 km.

Global Geopotential Models only provide height anomalies while for orthometric heights geoid undulations are required. This geoid-quasi geoid separation corrections are provided by the authors of EGM2008 and can reach a value of 3.5 m in the mountains in north Bhutan. However, since they assume a too coarse simplification of the topography, we have computed more accurate corrections using the algorithm of Flury and Rummel (2009) and the SRTM topography. The differences can reach the meter level.

Comparison of 27 GNSS/levelling benchmarks with DRUKGEOID15 and EGM2008 showed standard deviations of 0.55 and 1.70 m for both models respectively, showing the superiority of DRUKGEOID15. Furthermore, simulations using synthetic gravity data showed that the DRUKGEOID15 has an accuracy of around 10-20 cm.

The vertical datum of DRUKGEOID15 has been fixed to point TH01 in Thimphu. At this point the GNSS ellipsoidal height minus the geoid undulation is exactly equal to the official orthometric height of the point.

The DRUKGEOID15 geoid has been provided various digital formats for the following software: Trimble Total Control, Leica Geo Office and a stand alone geoid converter.

5.2 Recommendations

The new DRUKGEOID15 geoid model provides a large improvement in the available undulation geoid models for Bhutan. The average uncertainty is now about 5cm for most of the country, in particular on inhabited regions, where its use is more necessary. Nevertheless, there are still space for improvements, in particular at the border regions in the North, East and West. Therefore, it is recommended that more gravimetric/GNSS observations will be done in the North and in India from West to East, as well in some areas in the interior of Bhutan (cf. Figure 8 for the areas lacking observations) to better constrain the model in these areas. This will also improve the model in the rest of the country.

We also recommend that the DRUKGEOID15 geoid undulation model will be adopted as the official geoid model for Bhutan and that its use will be disseminated among all potential users, both at the public and private sectors. One suggestion is to publish it on the official web site of NLC.

6. Digital Annexes

All material produced during this project, namely observations, reports and models, are made available to NLC. In order to guarantee their permanent availability, this material is stored online in a cloud server. It can be accessed using the following link:

<https://www.dropbox.com/sh/g9yjf4yezg12c1j/AACaLtUgDFMbxWWms2ti jzHRa?dl=0>

Name	
▼ Documents	✓
▶ GravityGNSS_Fieldbook	✓
▶ NewTablesPlots	✓
BhutanCompleteGravObs.pdf	✓
BhutanGeoid.pptx	✓
ComparisonBenchmarks.xlsx	✓
GravimetricPoints_Coordinates_Bhutan_v20150731.xlsx	✓
GravimetricPoints_Coordinates_Bhutan.xlsx	✓
PosterDrukGeoid15.pptx	✓
Readme.txt	✓
SEGAL_Bhutan_Gravity_ReportA.1.pdf	✓
SEGAL_Bhutan_Gravity_ReportA.2.pdf	✓
SEGAL_Bhutan_Gravity_ReportA.CoverLetter.pdf	✓
▼ GeoidFiles	✓
DRUKGEOID15.bin	✓
DRUKGEOID15.ggf	✓
DRUKGEOID15.nc	✓
DRUKGEOID15.txt	✓
README.txt	✓
▼ GNSS	✓
▶ GNSSBaseStations	✓
▶ GNSSPointsPostFeb	✓
▶ GNSSPointsPreFeb	✓
▶ TH01	✓
Readme.txt	✓
▼ Gravity	✓
1010May212015.txt	✓
1010May212015.txt_ori	✓
1712Apr212015.txt	✓
1712Apr212015.txt_ori	✓
Jamphel.dat	✓
Jamphel2.dat	✓
Kinzang.dat	✓
Kinzang2.dat	✓
Readme.txt	✓
results_fourth.dat	✓
results_fourth.txt	✓
stations_Bhutan.dat	✓

Figure 28 – Structure of the folders inside the digital repository.

7. References

- Farr, T. G., P. A. Rosen, E. Caro, R. Crippen, R. Duren, S. Hensley, M. Kobrick, et al. 2007. "The Shuttle Radar Topography Mission." *Reviews of Geophysics* 45 (June): 2004. doi:[10.1029/2005RG000183](https://doi.org/10.1029/2005RG000183).
- Flury, Jakob, and Reiner Rummel. 2009. "On the geoid-quasigeoid separation in mountain areas." *Journal of Geodesy* – (February): 0–0. doi:[10.1007/s00190-009-0302-9](https://doi.org/10.1007/s00190-009-0302-9).
- Forsberg, R., and C.C. Tscherning. 1981. "The Use of Height Data in Gravity Field Approximation by Collocation." *J. Geophys. Res.* 86 (B9): 7843–54.
- Förste, Christoph, Sean Bruinsma, Richard Shako, Jean-Charles Marty, Frank Flechtner, Oleh Abrikosov, Christoph Dahle, et al. 2011. "EIGEN-6 - A new combined global gravity field model including GOCE data from the collaboration of GFZ-Potsdam and GRGS-Toulouse." *Geophysical Research Abstracts*, Vol. 13, EGU2011-3242-2.
- Moritz, Helmut. 1980. *Advanced Physical Geodesy*. Herbert Wichmann Verlag Karlsruhe, Abacus Press Tunbridge Wells Kent.
- Pavlis, N. K., S. A. Holmes, S. C. Kenyon, and J. K. Factor. 2012. "The development and evaluation of the Earth Gravitational Model 2008 (EGM2008)." *J. Geophys. Res.* 117: B04406. doi:[10.1029/2011JB008916](https://doi.org/10.1029/2011JB008916).
- Sjöberg, L. E. 2005. "A discussion on the approximations made in the practical implementation of the remove compute restore technique in regional geoid modelling." *J. Geod.* 78 (May): 645–53. doi:[10.1007/s00190-004-0430-1](https://doi.org/10.1007/s00190-004-0430-1).
- Smith, D. A. 1998. "There Is No Such Thing as 'the' EGM96 Geoid: Subtle Points on the Use of a Global Geopotential Model." *IGeS Bulletin, Milan* 8: 17–28.
- Tscherning, C. C., and R. H. Rapp. 1974. *Closed covariance expressions for gravity anomalies, geoid undulations, and deflections of the vertical implied by anomaly degree variance models*. 208. Ohio State University, Columbus, Ohio.
- Vaníček, P., R. Kingdon, and M. Santos. 2012. "Geoid versus quasigeoid: a case of physics versus geometry." *Contributions to Geophysics and Geodesy* 42 (January): 101–18. doi:[10.2478/v10126-012-0004-9](https://doi.org/10.2478/v10126-012-0004-9).

Annexes